XVI

CONGRESO INTERNACIONAL DEL VIDRIO
INTERNATIONAL CONGRESS ON GLASS
INTERNATIONALER GLASKONGRESS
CONGRÈS INTERNATIONAL DU VERRE

VOL. 2

Glass transition - Transition vitreuse - Glasübergang
Phase transformation - Transformation de phases - Phasenumwandlung
Non-oxide glasses - Verres sans oxygéne - Nichtoxidische Gläser

BOL. SOC. ESP. CERAM. VID. 31-C (1992) 2

CHEMICAL ASPECTS OF THE GLASS TRANSITION IN MIXED-ALKALI AND MIXED-NETWORK GLASSES

G.D.Chryssikos, J.A.Kapoutsis, M.S.Bitsis, E.I.Kamitsos, A.P.Patsis
Theoretical and Physical Chemistry Institute, National Hellenic Research Foundation
48, Vas. Constantinou Ave., 11635, Greece

A.J.Pappin
Department of Engineering, Aberdeen University, Aberdeen AB9 2UE, Scotland, U.K.

ABSTRACT

Glasses in the pseudobinary systems $xNaBO_2.(1-x)LiBO_2$ and $xLiAlO_2.(1-x)LiBO_2$ have been prepared and studied by vibrational spectroscopy and differential scanning calorimetry. The corresponding phase diagrams have been investigated and the crystals discovered formed the basis for the structural understanding of the glasses. The temperature and composition dependence of the glass devitrification products is used to decode the structural relaxations governing the melt to glass transition.

INTRODUCTION

A chemical assessment of the glass transition implies the establishment of equilibria between discrete entities in the melt and their kinetic freezing upon quenching. Recently, Mazurin forwarded a simple theoretical model on the temperature and time dependence of chemical equilibria and succeeded to reproduce phenomenological aspects of the glass transition (1). The microscopic experimental support to this approach is difficult, since structural data on melts are scarce, and the *in situ* probing of the structural changes occurring upon quenching unfeasible.

Nevertheless, the complicated thermodynamic and kinetic processes are stored in the structure of glass, which retains the memory of structural events that led to its formation (2). We have recently demonstrated the possibility to decode conveniently this memory by subjecting glasses to isothermal devitrification at temperatures both below and above T_g and evaluating spectroscopically the structure of the crystallization products. In the case study of glassy lithium metaborate, g-$LiBO_2$, we found evidence for the participation in the glass network of structural arrangements encountered in three distinct polymorphs: α-, β'- and γ-$LiBO_2$ (2). The vitrification of g-$LiBO_2$ was attributed to the entanglement of the $\alpha \rightarrow \beta' \rightarrow \gamma$ transformations in the melt upon quenching. The three $LiBO_2$ polymorphs exhibit different ratios of metaborate triangles and tetrahedra ($B\Phi_2O^-$ and $B\Phi_4^-$, respectively, where Φ and O denote bridging and terminal oxygen atoms). Hence, our results on the glass transition of $LiBO_2$ are compatible with the isomerization scheme proposed by Mazurin (1),

with the added value of novel structural understanding beyond the local range order (2,3).

This report deals with the application of devitrification/structural studies to systems more complex than glassy $LiBO_2$, namely the pseudobinary glass families $xNaBO_2.(1-x)LiBO_2$, $0 \le x \le 0.75$, and $xLiAlO_2.(1-x)LiBO_2$, $0 \le x \le 0.42$. The systems have been selected so as to represent a typical mixed-alkali system with fixed network stoichiometry, and a mixed-network situation with constant average charge per boron polyhedron.

EXPERIMENTAL

Glasses have been prepared conventionally, their Raman and infrared reflectance spectra have been obtained, and their Tg measured by DSC. Moreover, the crystalline phase diagrams corresponding to the glass forming regions have been studied in detail by melt crystallization, high temperature solid state reactions and glass devitrification.

RESULTS AND DISCUSSION

The compositional dependence of Tg for the two systems is shown in figure 1. Both $NaBO_2$ and $LiAlO_2$ substitutions result in a sharp initial drop of Tg up to $x \approx 0.25$. Beyond this point, Tg continues to drop at a reduced slope in the former system, but shows a definite increase in the latter. It is obvious that these trends reflect structural alterations induced by increasing x and thus, their elucidation can benefit from the structural investigation of the glasses. A convenient way to approach such structural changes is by considering shifts of the isomerization equilibrium between metaborate triangles and tetrahedra , $B\Phi_2O^- \rightleftharpoons B\Phi_4^-$ (2,4), resulting from Li-Na mixing or Al substitution. A detailed spectroscopic investigation aiming at the elucidation of such effects is reported elsewhere (5,6) and the main results are summarized here.

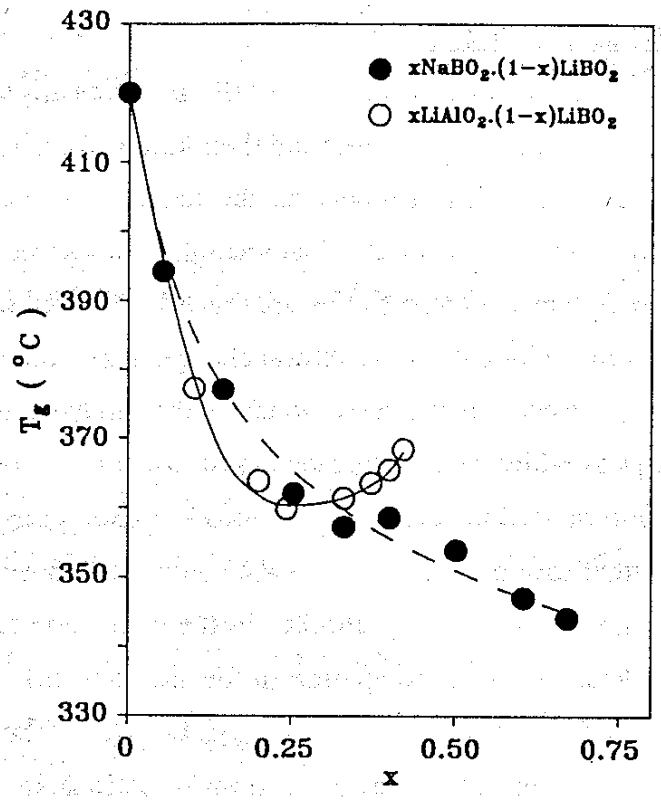

Figure 1. Glass transition temperatures of the $xNaBO_2.(1-x)LiBO_2$ and $xLiAlO_2.(1-x)LiBO_2$ glasses. Lines are guiding the eye.

Increasing x in Li-Na metaborate glasses results in the decrease of N_4, the fraction of four-coordinated boron atoms in the glass. This is directly inferred from the relative infrared intensity in the 800-1100 cm^{-1} region , where stretching vibrations of $B\Phi_4^-$ tetrahedra are active. As shown in figure 2, the characteristic

band envelopes in this range appear reduced in intensity as x increases (5). Figure 3 depicts the Raman spectra of Li-metaboroaluminate glasses, in which the spectral features of g-$LiBO_2$ are found to give place to bands at *ca* 400 and 950 cm^{-1}, which are typical of $Al\Phi_4^-$ tetrahedra (6).

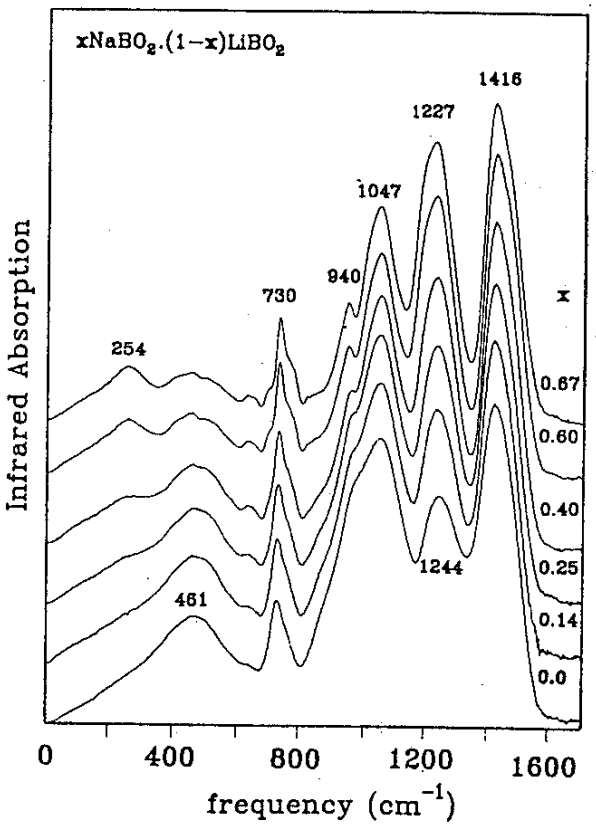

Figure 2. Infrared spectra of representative $xNaBO_2.(1-x)LiBO_2$ glasses.

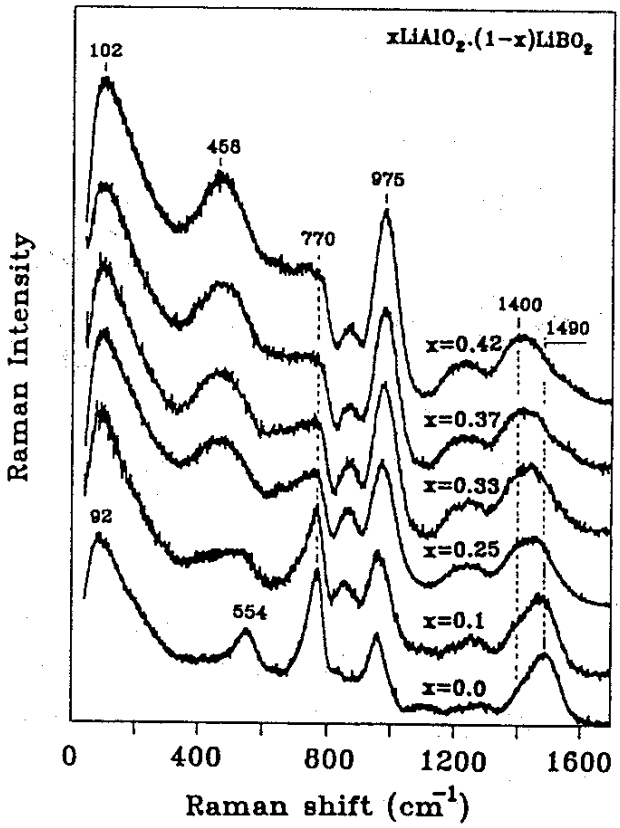

Figure 3. Raman spectra of representative $xLiAlO_2.(1-x)LiBO_2$ glasses.

Of particular interest in the structural investigation of borate glasses is the high frequency Raman region (1300-1600 cm^{-1}), where localized stretches of B-O^- bonds on metaborate triangles are active. The frequency maximum of this feature is sensitive to the second neighbours of the B-O^- probe which cause a redistribution of the π-electronic overlap, and can be correlated to the average B-O^- bond length (7). The regions of B-O^- Raman activity for representative glasses of the two families are compared in Figure 4. It is seen that increasing $NaBO_2$ substitution in $LiBO_2$ glass networks causes an upshift of the B-O^- stretching frequencies (fig. 4a), which indicates that the B-O^- probes sense a reduced number of $B\Phi_4^-$ second neighbours. Obviously, the result is compatible with the decrease of N_4 with x. To the contrary, increasing $LiAlO_2$ substitution results in a pronounced decrease of the average B-O^- stretch frequency (fig. 4b). This effect is taken to originate from the high basicity of $Al\Phi_4^-$ neighbours and manifests the covalent interactions between metaborate triangles and metaaluminate tetrahedra in the glass.

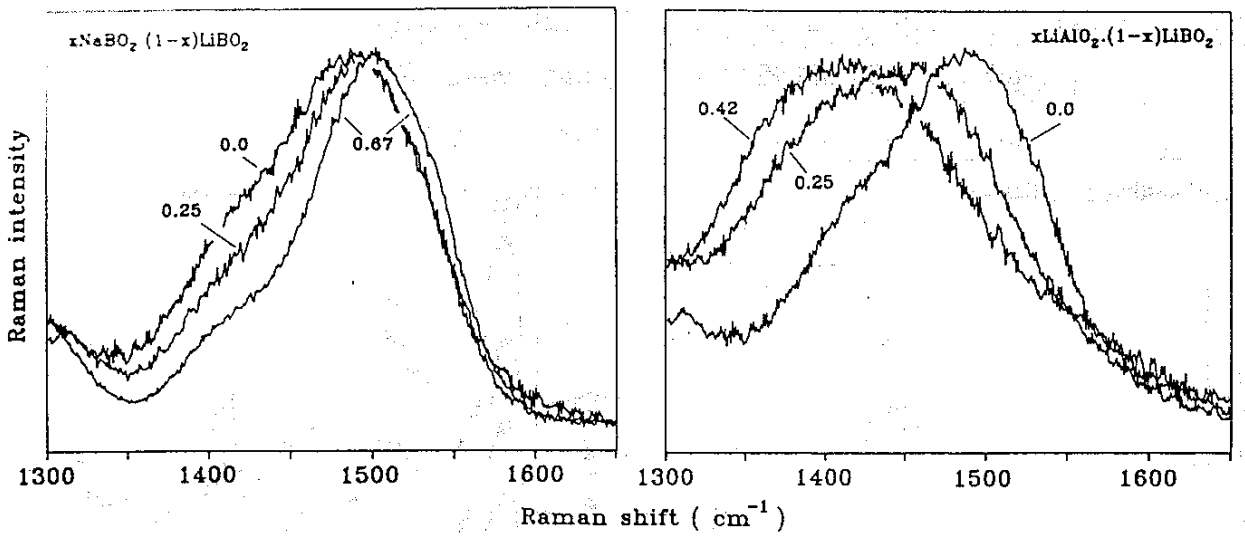

Figure 4. Representative Raman spectra of $xNaBO_2$-(1-x)$LiBO_2$ and $xLiAlO_2$-(1-x)$LiBO_2$ glasses in the frequency range of B-O stretching activity.

Further insight on the intermediate range structure of the glasses of interest comes from the study of the corresponding crystalline phase diagrams. The $LiBO_2$-$NaBO_2$ join is found to comprise three $LiBO_2$ polymorphs, a mixed alkali metaborate ($Li_3NaB_4O_8$), the well known ring-$NaBO_2$ compound and possibly a second $NaBO_2$ polymorph containing both triangles and tetrahedra (5). The corresponding $LiBO_2$-$LiAlO_2$ join contains, apart from the known polymorphs of the end-members, two mixed-network compounds with stoichiometries $Li_3B_2AlO_6$ and Li_2BAlO_4 (6). The former has been characterized by XRD techniques (8), while spectroscopic comparisons indicate that the latter is isostructural to its known Ca- and Sr- analogues (6,9). The crystal chemistry of the two systems shows a pronounced temperature dependence (polymorphic transitions, high temperature dissociation etc). Hence the study of the crystalline phase diagrams provides the thermodynamic driving force for structural rearrangements upon melt quenching. Moreover, examination of the glass spectra in light of those of the corresponding crystals reveals striking similarities and allows not only the identification of the network polyhedra, but also that of longer range arrangements in glass.

To investigate fully the chemical aspects of the glass transition in the two glass families, we have performed detailed devitrification experiments as a function of composition and temperature. It was first found that all Li-Na metaborate glasses, as well as the Li-metaboroaluminates with $x \leq 0.33$, exhibit sub-Tg crystallization. Under such mild conditions, devitrification proceeds presumably without major alterations of the glass network sequence (10), and hence the resulting crystalline products are structurally similar to the parent glasses. A second observation concerns the x dependence of the temperature ranges corresponding to β'-and γ-$LiBO_2$ formation. Pure glassy $LiBO_2$ devitrifies into β'-$LiBO_2$ between 400 and 420 °C and into γ-$LiBO_2$ below 400 °C (2).

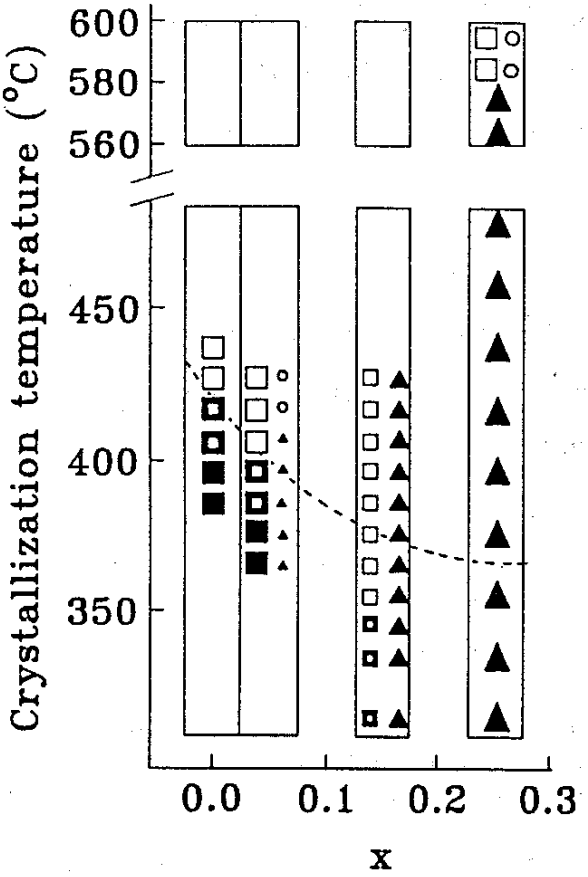

Figure 5. Temperature and composition dependence of the devitrification products of $xNaBO_2.(1-x)LiBO_2$ glasses with $0 \le x \le 0.30$. Symbols indicate the various crystalline products as follows: □ α-$LiBO_2$; ◘ β'-$LiBO_2$; ■ γ-$LiBO_2$; ○ ring-$NaBO_2$ and Δ $Li_3NaB_4O_8$ The size of the symbols depicts qualitatively their relative abundance in the products. The glass transition temperature of the samples is also indicated.

Additions of either $NaBO_2$ or $LiAlO_2$ suppress considerably these domains. Thus, a glass with x_{NaBO2} =0.05 devitrifies into β'-$LiBO_2$ between 380 and 400 °C and that with x_{NaBO2} =0.14 below 350 °C (5). The glass with x_{LiAlO2} =0.10 yields β'-$LiBO_2$ only below 375°C (6). Figure 5 gives a qualitative mapping of the devitrification products of $xNaBO_2.(1-x)LiBO_2$ compositions with $x \le 0.25$. In the case of glassy $LiBO_2$ the glass formation was associated with the entanglement of structural relaxations of the cooling melt, and the glass transition was correlated with the temperature threshold below which devitrification yields tetrahedra-containing polymorphs (2). In low x glasses ($x<0.25$) of either system, the growth of $LiBO_2$ polymorphs governs the devitrification profile for stoichiometric reasons. Thus, the systematic decrease with x of the α to β' devitrification temperature threshold can provide a structural account for the parallel decrease of Tg and the aforementioned similarity in the Tg vs x trends. Beyond x=0.25 the differences in crystal chemistry between the two systems set in and account for the deviation of the two curves from each other (figure 1).

While the devitrification chemistry of g-$LiBO_2$ and its low-substitution pseudobinary derivatives is structurally discontinuous around Tg, that of glasses with x_{NaBO2}=0.25 and x_{LiAlO2} =0.33 and 0.50 is structurally smooth. This is taken to indicate that the chemical relaxations of the melt to glass transition in the latter cases do not involve major alterations of the network structure and should induce a smoother increase of the log viscosity upon approaching Tg. Thus, while $LiBO_2$ is

a melt in the fragile limit (11), increasing either x_{NaBO2} or x_{LiAlO2} results in the enhancement of the melt's strength. At the same time the definition of chemically identifiable pseudophases in glass (3) becomes less meaningful (5,6). It should also be added that the above spectroscopic and devitrification results confirm the fact that the network structure of mixed alkali glasses should not be taken as independent of alkali-mixing (12,13).

Acknowledgements: Helpful discussions with Drs. M.D.Ingram and J. Hutchinson (AU) are acknowledged. The work has been financed by NHRF and AU. Collaboration between the two laboratories was made possible by the NHRF / Royal Society Exchange Programme, as well as by the British Council Academic Travel Grant ATH/609/3/30.

REFERENCES

1. O.V.MAZURIN, J.Non-Cryst. Solids: Theory of glass transition, Chemical equilibria approach. **129** (1991) 259.
2. G.D.CHRYSSIKOS, E.I.KAMITSOS, A.P.PATSIS, M.S.BITSIS and M.A.KARAKASSIDES, J.Non-Cryst. Solids:The devitrification of Lithium metaborate, Polymorphism and glass formation. **126**, (1990) 42, and Chemical relaxations at the glass transition of a lithium conducting glass. **131-133** (1991) 1068
3. M.D.INGRAM, G.D.CHRYSSIKOS and E.I.KAMITSOS, J.Non-Cryst. Solids: Evidence from vibrational spectroscopy for cluster and tissue pseudophases in glass. **131-133** (1991) 1089
4. E.I.KAMITSOS, M.A.KARAKASSIDES, A.P.PATSIS and G.D.CHRYSSIKOS, J.Non-Cryst. Solids. Laser-induced crystallization of glassy caesium metaborate studied by Raman spectroscopy. **116** (1990) 115.
5. G.D.CHRYSSIKOS, J.A.KAPOUTSIS, A.P.PATSIS, E.I.KAMITSOS and A.J.PAPPIN, J.Non-Cryst. Solids. Lithium-sodium metaborate glasses, structural aspects and vitrification chemistry, submitted for publication (1992)
6. G.D.CHRYSSIKOS, M.S.BITSIS, E.I.KAMITSOS and A.J.PAPPIN, manuscript in preparation.
7. G.D.CHRYSSIKOS, J.Raman Spectroscopy. Bond length-Raman frequency correlations in borate crystals. **22** (1991) 645.
8. G.K.ABDULLAEV and K.S.MAMEDOV, Sov. Phys. Crystallogr. Refinement of the crystal structure of lithium aluminoborate $Li_6[Al_2(BO_3)_4]$. **27** (1982) 229.
9. K.FUKUMI, J.FUKUNAGA, N.YOSHIDA and M.IHARA, Yogyo-Kyokai-Shi. Raman spectroscopic study of $CaO\text{-}Al_2O3\text{-}B_2O_3$. **92** (1984) 680.
10. U.GIESE, H.HESSENKEMPER and R.BRUKNER, J.Non-Cryst. Solids. Crystallization behaviour of $CaBa(PO_3)_4$ glass depending on temperature and load. **127**, 75 (1991)
11. C.A.ANGELL, C.A.SCAMEHORN, D.J.LIST and J.KIEFFER, Proc. X Int. Congr. Glass. Glassforming liquid oxides at the fragile limit of the viscosity-temperature relationship. Leningrad 1989, Vol. 1a, p. 204
12. A.H.DIETZEL, Phys. Chem. Glasses. On the so-called mixed alkali effect. **24** (1983) 172
13. E.I.KAMITSOS, A.P.PATSIS and G.D.CHRYSSIKOS, Phys. Chem. Glasses. Interactions between cations and the network in mixed alkali borate glasses. **32** (1991) 219.